ELSEVIER

Physica C 278 (1997) 213–222

PHYSICA C

Penetration depth and conductivity of NbN and $DyBa_2Cu_3O_{7-\delta}$ thin films measured by mm-wave transmission

B.J. Feenstra [a,*], F.C. Klaassen [a,1], D. van der Marel [a], Z.H. Barber [b], R. Perez Pinaya [c], M. Decroux [c]

[a] *Materials Science Centre, Laboratory of Solid State Physics, University of Groningen, Nijenborgh 4, 9749 AG Groningen, The Netherlands*

[b] *Department of Materials Science and Metallurgy, University of Cambridge, Pembroke Street, Cambridge CB2 3QZ, UK*

[c] *Département de Physique de la Matière Condensée, University of Geneva, 24, quai Ernest-Ansermet, CH-1211 Genève 4, Switzerland*

Received 3 January 1997; revised 21 March 1997

Abstract

Using mm-wave transmission, information about both the real and imaginary part of the dielectric function of superconducting thin films is obtained. This is done by fitting the Fabry–Perot resonance spectrum for the film plus substrate over a broad frequency range (110–180 GHz) using the full Fresnel equations and a two-fluid description for the dielectric function. Depending on the thickness of the film, the transmission is mainly determined by $\epsilon'(\sim 1/\lambda^2)$ or $\epsilon''(\sim \sigma_1)$. For NbN a behaviour consistent with the BCS-formalism is found. For $DyBa_2Cu_3O_{7-\delta}$, results on films of thicknesses ranging from 20 to 80 nm are presented. We find a T^2 dependence of the penetration depth at low temperatures and a strongly enhanced conductivity below T_c, indicative of a strong reduction of the quasiparticle scattering. For the 20 nm film the transmission is dominated by ϵ'', even down to 60 K. © 1997 Elsevier Science B.V.

PACS: 74.25.Gz; 74.25.Nf; 74.76.Bz
Keywords: Thin films; Penetration depth; mm-wave spectroscopy

1. Introduction

In the process of establishing the symmetry of the order parameter of the high temperature superconductors, electrodynamical properties such as the penetration depth (λ) and the conductivity (σ_1) are playing a major role. Most contemporary results on the temperature dependence of λ have been obtained at microwave frequencies using a resonant cavity in a perturbative mode [1–3]. At temperatures lower than 40 K, Hardy et al. [1] observed a linear temperature dependence in a $YBa_2Cu_3O_{6.95}$ single crystal using a loop-gap resonator at 1 GHz. This dependence was predicted to exist for a superconductor having lines of nodes in the gap function, as for instance in case of a d-wave symmetry [4]. The unconventional pairing symmetry has been confirmed by other techniques and properties [5–9] and it is now generally accepted, although consensus has not been reached about the exact symmetry.

* Corresponding author. Tel.: +31 50 3634780; fax: +31 50 3634825; e-mail: feenstra@optics.phys.rug.nl.

[1] Present address: Vrije Universiteit, Faculty of Physics and Astronomy, De Boelelaan 1081, 1081 HV Amsterdam, The Netherlands.

PII S0921-4534(97)00124-X

The linear behaviour, believed to be intrinsic, was however initially never observed in thin films. Several groups found other dependencies ranging from T^2 to exponential [10–13], presumably originating from extrinsic sources such as resonant impurity scattering or weak links [4,14,15]. Indeed, in case of a d-wave superconductor, it has been shown theoretically that extrinsic scattering sources can turn the linear temperature dependence into a T^2 dependence [4,14]. De Vaulchier et al. [16] were the first to report the linear dependence in a $YBa_2Cu_3O_{7-\delta}$ thin film using mm-wave transmission. They also noticed a correlation between the observation of a large λ_L and the T^2 dependence, using the absolute information obtained by this technique. The correlation was interpreted as evidence for the extrinsic nature of the nonlinear dependence, for example due to weak links [15].

Other unconventional behaviour at mm-wave frequencies has been observed in the conductivity σ_1 [17–19]. Unlike the reduced σ_1 expected for a BCS-superconductor, the conductivity is largely enhanced upon entering the superconducting state, showing a broad peak at temperatures ranging from 30 to 70 K. The peak shows some similarities with a BCS-coherence peak [20,21], however, the absence of a Hebel–Slichter peak in NMR-data and the strong frequency dependence of both its amplitude and position are indications that an alternative explanation should be used. In particular, the maximum in σ_1 for the cuprates has been interpreted as originating from an anomalously strong reduced scattering rate (γ) below T_c, such that the conductivity increases despite the decreasing quasiparticle density. Using Zn-doping in $YBa_2Cu_3O_{6.95}$ single crystals, Bonn et al. [22] were able to show that the maximum in the conductivity is reduced if the disorder in the material is increased, since the drop in γ is then limited by the residual scattering. The strong reduction of γ indicates that ordinary electron phonon scattering cannot be the main quasiparticle scattering mechanism. This is supported further by the linear temperature dependence of the DC resistivity in the normal state for the optimally doped material, indicating that the 'normal' state does not follow ordinary Fermi liquid predictions.

Measuring thin films using the aforementioned resonant cavity technique is usually rather complicated, since the only option one has is to utilize the film as the cavity endplate. This inevitably leads to leakage, thereby complicating the analysis. It will be shown in the course of this paper that measuring the mm-wave transmission through a thin film can be a good alternative for measuring the electromagnetic properties. In fact, one is able to obtain absolute information on both the real and imaginary part of the dielectric function [23]. Moreover, by selecting the proper film thickness we can control the sensitivity such that either the conductivity (σ_1) or the superfluid density ($\sim 1/\lambda^2$) dominates the temperature dependence of the transmission. It will be shown that for certain values of the London penetration depth λ_L and the conductivity σ_1, one can choose the film thickness such that even in the super-conoducting state down to low temperatures (~ 60 K) the influence of the superfluid density is insignificant.

2. Experimental

Our experimental setup is shown in Fig. 1. As a source we use a Backward Wave Oscillator (BWO), having a broad frequency response ranging from 110 to 180 GHz, making scans as a function of frequency feasible. The radiation is first coupled into a waveguide, through a modulator and a calibrated attenuator. The former creates the AC response necessary for the detector, while the latter is used to maintain the signal level comparable during three sequential measurements, i.e. thin film on substrate, bare substrate and reference aperture. This ensures that the response of the detector is linear over the full frequency range. The radiation is then coupled out of the waveguide using a Gaussian horn, and treated quasi-optically thereafter. We use a parabolic mirror, placed slightly out of focus to make a 3:1 image at the centre of the cryostat (1.5–300 K) where the superconducting thin film is situated. Another parabolic mirror is used to make a second focus (1:1) which can be utilized for room temperature measurements. Eventually the beam is focused onto either one of two detectors, a highly sensitive liquid ^{4}He cooled Si-bolometer, or a fast waveguide diode detector.

The NbN-film of 55 nm thickness was deposited on an MgO substrate using DC reactive magnetron

sputtering. This was done in a gas composition of 3.0% CH_4/30.0% N_2/Ar, at a temperature of approximately 840°C [24]. T_c was enhanced to 16.5 K, by the inclusion of carbon. The resistivity ratio (16.5 K/300 K) was close to unity.

The $DyBa_2Cu_3O_{7-\delta}$ films of thicknesses ranging from 20–80 nm, were deposited by RF sputtering on $LaAlO_3$ substrates using the (100) surface. The substrate temperature was 745°C while a mixture of argon and oxygen gas was used, at pressures of 105 and 45 mTorr respectively. After the deposition the samples were annealed in 200 mTorr oxygen for 30 min at 450°C. The quality of the surface was checked with X-ray diffraction, which showed very good crystallization. Due to the high crystallinity of the films, the oxygen diffusion process was rather slow, resulting in a somewhat reduced T_c (88 K) for one of the films (20 nm).

During measurements three sequential scans as a function of frequency are taken at a fixed temperature: thin film on substrate, bare substrate and reference aperture. The latter is used to yield absolute transmission coefficients for both sample and substrate, which are then used in the remainder of the analysis. The transmission through a two layer system is given by the Fresnel equations:

$$t = \frac{\tau_{02} e^{i\psi} t_{20}}{1 - r_{20}\rho_{20} e^{2i\psi}}, \quad \psi = \frac{2\pi\nu d_s p}{c} \tag{1}$$

where ν is the frequency of the incident radiation, p is the complex index of refraction of the substrate, d_s is the thickness of the substrate and:

$$\tau_{02} = t_{01} e^{i\phi} \frac{1}{1 - r_{10} e^{i\phi} r_{12} e^{i\phi}} t_{12}, \tag{2}$$

$$\rho_{20} = r_{21} + t_{21} e^{2i\phi} r_{10} \frac{1}{1 - r_{10} e^{i\phi} r_{12} e^{i\phi}} t_{12}. \tag{3}$$

Here $\phi = 2\pi\nu d_f \sqrt{\epsilon}/c$ is a complex phase, ϵ is the dielectric function of the film and d_f is the film-thickness. The reflection and transmission coefficients at each interface are:

$$r_{ij} = \frac{n_i - n_j}{n_i + n_j}, \quad t_{ij} = \frac{2n_i}{n_i + n_j}. \tag{4}$$

The multiple reflections in the substrate are incorporated in the phase factor $e^{i\psi}$, while a similar contribution from the film is included in a phase factor $e^{i\phi}$, incorporated in the transmission and reflection coefficients τ_{02} and ρ_{20}.

First, the interference pattern of the substrate is used to obtain its full dielectric function ($\tilde{n} = n + ik$) at each temperature. In Fig. 2 the transmission of a $LaAlO_3$ substrate is shown together with the obtained fit. Subsequently, we continue by modeling the transmission through the sample using the full Fresnel equations, the measured optical constants of

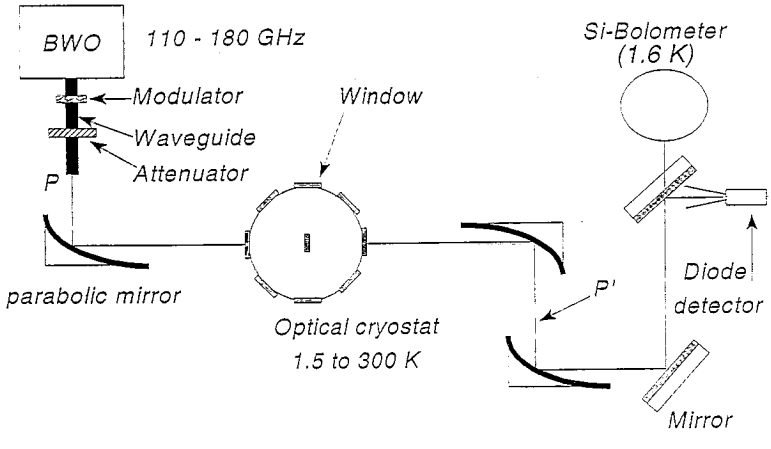

Fig. 1. Experimental setup.

the substrate and a two-fluid model for the dielectric function of the film:

$$\epsilon = \epsilon_\infty - \frac{\nu_{pn}^2}{\nu(\nu + i\gamma(T))} - \frac{c^2}{(2\pi)^2 \nu^2 \lambda^2(T)}. \quad (5)$$

Here ν_{pn} is the normal state plasma frequency, $\gamma(T)$ is the scattering rate, $\lambda(T)$ is the penetration depth and ν is the measurement frequency. We recall that $\epsilon'' = 2\sigma_1/\nu$ above T_c, and $\sigma_1 \to 1/\rho_{dc}$ for low frequencies. Furthermore, $\epsilon' = -c^2/(\nu\lambda)^2$ at low temperatures and is therefore directly related to the superfluid density of the material. For the measurements presented in this paper, the scattering rate γ remains larger than the measurement frequency ν, so that λ and σ_1 have only a weak frequency dependency. mm-Wave experiments under conditions where $\nu > \gamma$ have been reported by Dähne et al. [25].

In order to see the influence of ϵ' and ϵ'' on the transmission and its temperature dependence, we consider the idealized but nevertheless instructive case of a free standing film in the limit that $|2\pi\nu d\epsilon/c| \ll 1$. The transmission is then given by

$$T = \left(1 + \left(\frac{2\pi\nu d\epsilon''}{c}\right) + \left(\frac{\pi\nu d\epsilon'}{c}\right)^2\right)^{-1} \quad (6)$$

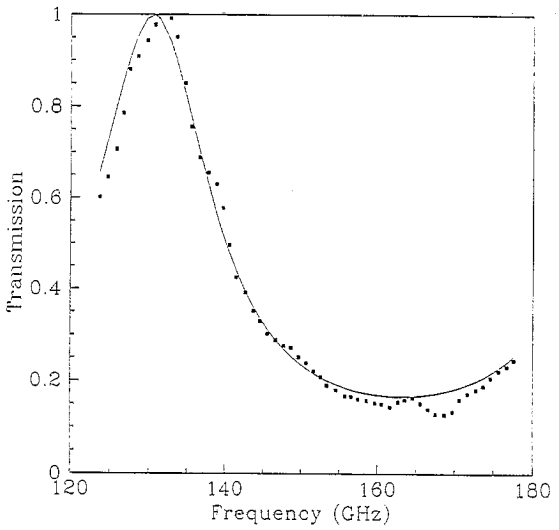

Fig. 2. The transmission through a bare $LaAlO_3$ substrate at room temperature, showing its Fabry–Perot resonance. The optical constants used for the fit were: $n = 4.70$ and $k = 0$.

where d is the film thickness. From this expression it is evident that the thickness plays an important role in determining the relative significance of the real and imaginary parts. For very thin films the absorptive term ($\sim \epsilon''$) will dominate, while for thicker films, the reactive term ($\sim \epsilon'$) will be most significant. From Eq. (6) one can estimate a crossover thickness (d_c):

$$d_c = \frac{2c\epsilon''}{\pi\nu(\epsilon')^2}. \quad (7)$$

Since the magnitudes of both contributions ϵ' and ϵ'' are very different for a normal metal or a superconductor (due to the presence of the superfluid), d_c will be different for the two cases. Assuming that $\nu^2 \ll \gamma^2$, we find that for a metal $d_c \approx 2c\gamma^3\pi^{-1}(\nu\nu_{pn})^{-2}$, while for a superconductor $d_c \approx 32\pi^3\nu_{pn}^2\nu^2\lambda^4c^{-3}\gamma^{-1}$. Taking common values for 123-superconductors ($\gamma = 100$ cm^{-1}, $\nu = 5$ cm^{-1}, $\nu_{pn} = 10^4$ cm^{-1} and $\lambda = 2000$ Å), we obtain that $d_c \sim 2.5$ μm in the normal state, while $d_c \approx 0.4$ Å for $T \ll T_c$. Consequently, for most thin films the transmission in the normal state will be determined by σ_1, while in the superconducting state it will be determined by λ. Equivalently, by fixing the thickness and using the temperature dependence of the sample properties one can estimate the temperature range at which both contributions will be equally important. This will be shown in a more specific analysis using the measured values for $DyBa_2Cu_3O_{7-\delta}$, given in the following section.

3. Results

In order to check the reliability of the technique we began by first measuring a conventional superconductor (NbN) to make sure that we would be able to resolve the intrinsic properties of the thin film. In Fig. 3 the transmission of the NbN film on an MgO substrate is shown as a function of frequency, for several temperatures, both above and below T_c. The peak in the interference spectrum is determined by the MgO substrate, having $n = 3.43$ and $k = 0$. We are able to fit the spectra using the Drude description of Eq. (5). As expected for a metallic film, $\epsilon'' \gg |\epsilon'|$, while in the superconducting state the opposite is

valid, $|\epsilon'| \gg \epsilon''$. For the fit we have focused our attention on the main peak around 135 GHz. Notice, furthermore, that the interference pattern shows no major changes besides the reduced amplitude in the superconducting state.

Plotting the temperature dependence at one particular frequency (140 GHz) as shown in the inset of Fig. 3, the dramatic change in transmission at T_c is more easily observed. The temperature dependence of the transmission coefficient can be fitted very well using the assumptions that $\lambda(T)$ can be described by the Gorter–Casimir relation [26], $\sigma_1(T)$ follows the Mattis–Bardeen relations [27] and $2\Delta/k_BT = 4.0$. The only adjustable parameters used in the calculation were the normal state conductivity ($\sigma_1(1.7\,\mathrm{K}) = 15\,000\ \Omega^{-1}\,\mathrm{cm}^{-1}$) which determines the absolute transmission at 17 K, and the London penetration depth ($\lambda_L = 400$ nm) which determines the transmission coefficient at low temperatures. Although this penetration depth is somewhat higher than the lowest reported values of about 100 nm [28], there is considerable variation in the literature due to a wide range of film structures.

In Fig. 4 the transmission through a 20 nm thick $DyBa_2Cu_3O_{7-\delta}$ film on a $LaAlO_3$ substrate is shown. Similar results as presented below have been reproduced on a different batch of films. The interference pattern of the substrate at room temperature was shown already in Fig. 2. From this $n = 4.70$ and $k = 0$ was obtained. As expected, the optical constants are temperature independent for the perovskite substrate. The additional oscillations present in the transmission are caused by internal reflections within the sample-holder. Due to the slightly modified standing wave pattern, these do not cancel completely after division by the transmitted signal through a reference hole.

In contrast to the results for the NbN film, the interference pattern of a $DyBa_2Cu_3O_{7-\delta}$ thin film changes dramatically when the temperature is low-

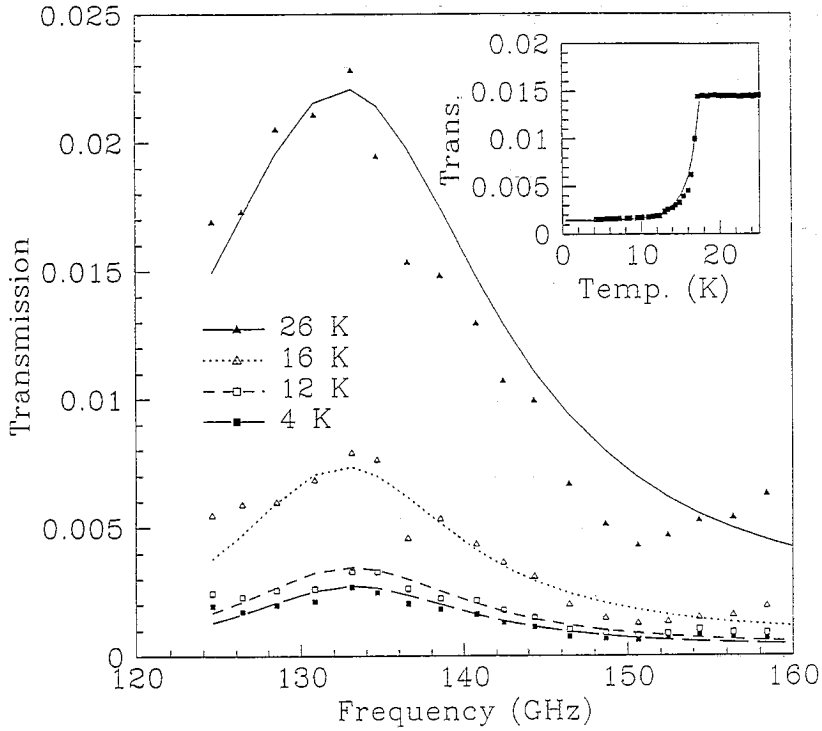

Fig. 3. Transmission through NbN on MgO (thickness = 55 nm, $T_c = 16.5$ K) for 4 different temperatures together with their fit (4 K: solid squares, 12 K: open squares, 16 K: open triangles and 26 K: solid triangles). Inset: temperature dependence at 140 GHz together with a BCS-fit using $\sigma_1(17\,\mathrm{K}) = 15\,000\ \Omega^{-1}\,\mathrm{cm}^{-1}$ and $\lambda_L = 400$ nm.

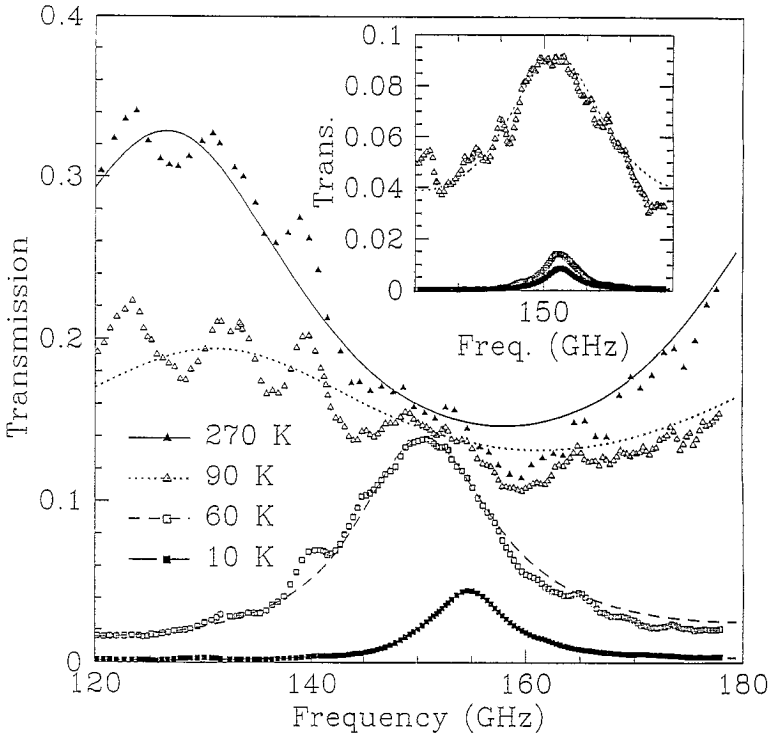

Fig. 4. Transmission through $DyBa_2Cu_3O_{7-\delta}$ on $LaAlO_3$ (thickness = 20 nm, T_c = 88 K) for 4 different temperatures together with their fit (10 K: solid squares, 60 K: open squares, 90 K: open triangles and 270 K: solid triangles). Inset: Transmission of $DyBa_2Cu_3O_{7-\delta}$ (d = 34 nm) for three different temperatures (10, 60 and 90 K).

ered. This is due to the stronger change in conductivity of the film, thereby altering the matching of the impedances of both film and substrate. This effect can be demonstrated by modeling the transmission through a similar stratified system, changing either the optical conductivity σ_1 of the film, keeping the thickness fixed at 20 nm (Fig. 5a), or by altering its thickness at a fixed conductivity of 3000 Ω^{-1} cm^{-1} (Fig. 5b). Both parameters will have a similar effect on the transmission since this is mainly affected by their product. For a certain set of parameters the interference effect disappears completely, showing that the light passes only once through the substrate. Additionally, the magnitude of the dielectric function matching this requirement determines the absolute value of transmission at the turning point. This model calculation illustrates furthermore that one has to be careful with the interpretation of transmission curves measured as a function of temperature at a fixed frequency. A curve taken at 130 GHz will show a much larger temperature dependence than a curve

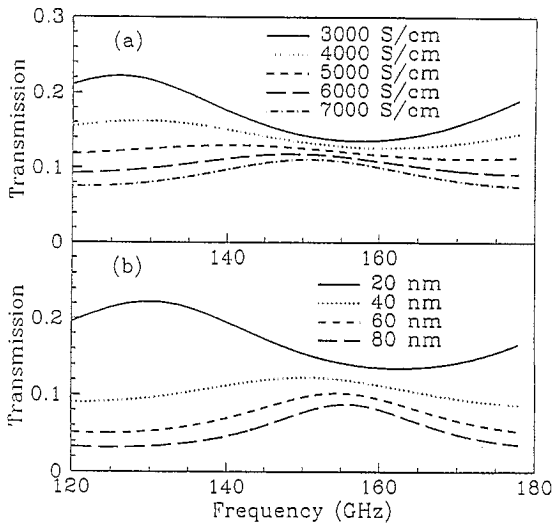

Fig. 5. Calculated transmission through a layered system (thin film on a substrate) as a function of conductivity (a), or thickness (b). For the substrate, the optical constants of $LaAlO_3$ were used (n = 4.70 and k = 0), while the film thickness for (a) was 20 nm and the conductivity for (b) was 3000 Ω^{-1} cm^{-1}.

taken at 150 GHz, although they will yield the same intrinsic film properties, once interference effects are taken into account.

At 150 GHz the transmission is nearly constant at temperatures higher than 60 K. At lower temperatures the amplitude of the interference peak drops and its width decreases rapidly. The transmission for the 34 nm film is depicted in the inset of Fig. 4 for the same temperatures as the 20 nm film (90, 60 and 10 K). The reduction in transmission at intermediate temperatures is much larger in the thicker film. As argued below, this is due to the stronger contribution of the superfluid in the 34 nm film. The transmission data for the 80 nm film show qualitatively similar behaviour.

To fit the transmission data presented in Fig. 4 two different approaches are used. First we start in the normal state, knowing that there is no superfluid fraction present (approach A). This yields both ϵ' and ϵ'', where the sensitivity in the metallic case is most extensive for $\epsilon''(\sim \nu_{pn}^2/\gamma)$. This approach is continued even when the sample is cooled below T_c where the addition of a superfluid contribution does not influence the fit for the 20 nm film significantly. We proceed until the peak becomes too narrow and fitting is no longer possible. The second approach (B) is to start at the lowest possible temperature (5 K) and assume that the superfluid fraction is the dominant contribution. We proceed to higher temperatures until the peak starts to broaden and the maximum remains nearly constant, thus inhibiting fitting with the superfluid as the only contribution. Obviously there will be a temperature range for which both terms are comparable, in which case a quantitative description is more complicated.

In Fig. 6a σ_1 is shown, while in Fig. 6b the total ϵ', including the superfluid contribution, has been depicted. Both quantities have been determined at

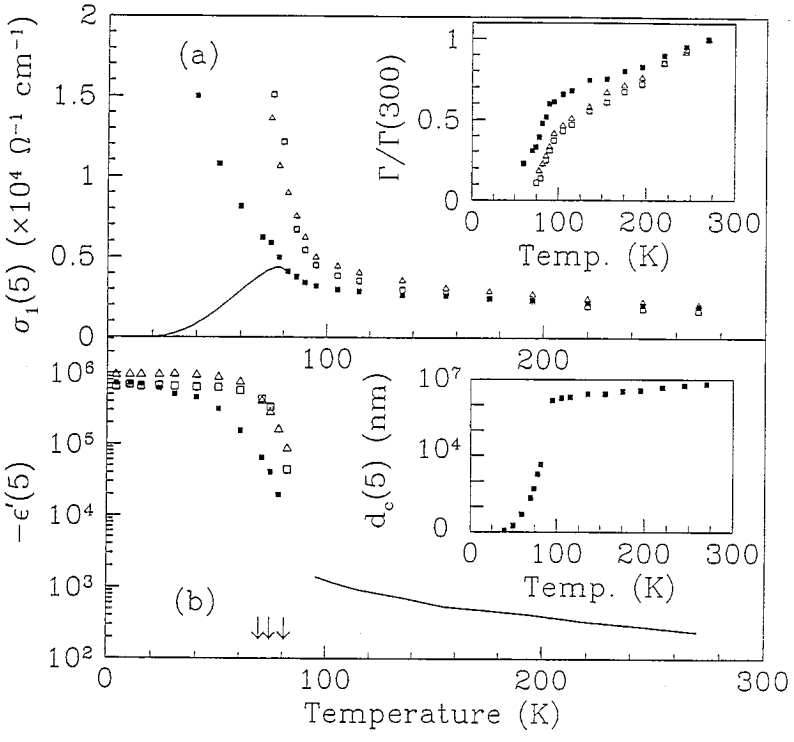

Fig. 6. (a) Temperature dependence of σ_1 for three $DyBa_2Cu_3O_{7-\delta}$ films with different thicknesses (20 nm: solid squares, 34 nm: open triangles and 80 nm: open squares). The normalized conductivity for a BCS-superconductor having a T_c of 92 K is included as the solid line. The inset shows γ, normalized to its RT-value. (b) Temperature dependence of ϵ'. The arrows indicate the temperatures where the critical thickness, d_c (inset), is approximately equal to the film thickness (20, 34 and 80 nm from left to right). All quantities have been calculated at the center frequency, $\nu = 5$ cm^{-1}.

the centre frequency, $\nu = 5$ cm^{-1}, using $\sigma_1 = \nu_{pn}^2 \gamma(\nu(\nu^2+\gamma^2))^{-1}$ and $\epsilon' = -\nu_{pn}^2(\nu^2+\gamma^2)^{-1} - c^2(2\pi\nu\lambda)^{-2}$. To determine σ_1, the values for ν_{pn} and γ were used, obtained from the fit following approach A. The solid curve in Fig. 6b corresponds to an estimate of ϵ' based on the expression $\epsilon' = -2\sigma_1/\gamma$ which is valid for the Drude model. In the inset of the upper panel the normalized scattering rate is depicted. Below T_c, σ_1 exhibits a rapid increase for all films. For comparison, the conductivity for a BCS-superconductor with a T_c of 92 K is included in the upper panel (solid line). The conductivity was normalized to the value of σ_1 for $DyBa_2Cu_3O_{7-\delta}$ at 92 K. This emphasizes the strikingly different behaviour of the high T_c superconductor. Similar behaviour has been observed before in $YBa_2Cu_3O_{7-\delta}$ [17,18], and is taken to be evidence of a rapidly suppressed scattering rate γ below T_c. Since, within the model used, $\sigma_1 \sim \nu_{pn}^2/\gamma$, two competing effects determine its temperature dependence. Below T_c the density of normal carriers will be reduced thereby reducing the plasma frequency, ν_{pn}, while the scattering of quasiparticles will also be reduced when the temperature is lowered. Having two different temperature dependencies produces a maximum in the conductivity. This maximum also resembles, superficially, a BCS coherence peak but shows a different temperature and frequency behaviour.

The total dielectric response, ϵ', is mainly determined by the superfluid contribution. For the 20 nm film ϵ' can not be determined accurately from 50 to 90 K, caused by the insensitivity of the transmission to ν_{ps} in this range.

Knowing the approximate values for the dielectric properties we return to Eq. (7) in order to show that the earlier claim that the sensitivity shifts from $\sigma_1(T)$ to $\lambda(T)$ in this temperature range was valid. Using Eq. (7) and the measured values for σ_1 and ϵ', the critical thickness was calculated. The result can be seen in the inset in the lower panel of Fig. 6. Since the values used to calculate d_c are intrinsic material properties the curve looks similar using the dielectric properties obtained for the 34 and the 80 nm film. Hence, it can be estimated at which temperature the critical thickness is approximately equal to the film thickness. These temperatures have been indicated in Fig. 6b by three arrows, where the thinnest film is represented by the lowest temperature. Around these temperatures both approaches A and B are inefficient, resulting in a larger uncertainty in the obtained absolute values of both σ_1 and ϵ'.

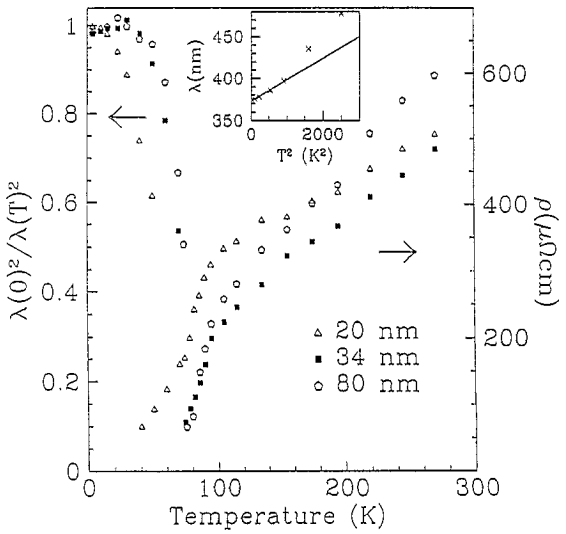

Fig. 7. Temperature dependence of the resistivity (right hand side) and the superfluid density $\lambda(0)^2/\lambda(T)^2$ (left hand side) for three $DyBa_2Cu_3O_{7-\delta}$ films with different thicknesses. (20 nm: triangles, 34 nm: squares and 80 nm: diamonds). In the inset the temperature dependence of the penetration depth is shown for the 20 nm film. The open symbols are obtained using approach A, while the close symbols result from approach B.

More results of the fitting procedure are displayed in Fig. 7 for all three films. The resistivity ρ is shown on the right hand side, while on the left hand side of Fig. 7 the superfluid density ($\lambda(0)^2/\lambda(T)^2$) is plotted. The results at low temperatures have been obtained using approach B. At higher temperatures ρ has been calculated by direct inversion of σ_1 obtained using approach A, assuming that σ_2 can be neglected. The DC resistivity obtained on samples prepared under identical conditions showed $\rho(300) = 650$ $\mu\Omega$ cm and $\rho(T_c) = 230$ $\mu\Omega$ cm, which is in good agreement with the mm-wave data in Fig. 7. In the normal state the mm-wave data show a linear temperature dependence of the resistivity, similar to the DC behaviour. However, the slope tells us that there is a fairly large residual scattering. For instance for the 20 nm film the intercept at $T = 0$ K is about 225 $\mu\Omega$ cm. Moreover, the slope is about twice as large as values measured for single crystals (1.05

$\mu\Omega$ cm/K vs. 0.45 $\mu\Omega$ cm/K), indicating that the difference cannot be explained by merely adding a temperature independent residual resistivity term.

The absolute penetration depth of the 20 nm film is shown in the inset of Fig. 7. The penetration depth shows a T^2-dependence at lower temperatures and a rather large λ_L of 370 nm. The other films show similar behaviour with a slightly different zero temperature penetration depth (325 and 360 nm for the 34 and 80 nm films respectively). Similar behaviour was observed before by de Vaulchier et al. [16] and was taken to be evidence for the extrinsic nature of the temperature dependence, due to the existence of weak links within the film. This provides additional evidence for the d-wave scenario, where the power-law temperature dependence of λ is lifted to a higher order by the presence of additional scattering. The slope of the quadratic curve (~ 0.025 Å/K^2) is about the same as that reported for one of the films in Ref. [16], although due to the extrinsic nature of the phenomenon there is no need for these values to be the same.

4. Conclusions

mm-Wave transmission can be used as a complimentary technique to characterize and study superconducting thin films on a fundamental level. From the NbN-data we see that we are able to resolve the intrinsic behaviour and obtain absolute values for both the real and imaginary part of the dielectric function and deduce values for σ_1 (15 000 Ω^{-1} cm^{-1}) and λ_L (400 nm). The temperature dependence follows the expected BCS-behaviour.

Furthermore, the transmission through $DyBa_2Cu_3O_{7-\delta}$ films of different thickness (20, 34 and 80 nm) was studied. An enhanced conductivity going into the superconducting state was observed, indicative of a large reduction in the scattering rate γ just below T_c. For the resistivity in the normal state, the linear behaviour typical for the cuprates was found. From the intercept at $T = 0$ K we learn that there is an additional residual scattering in the film, probably due to the same oxygen deficiency that reduces T_c slightly. The London penetration depth is fairly large for all films (325–370 nm), and has a T^2 dependence, consistent with a d-wave symmetry picture plus an additional extrinsic scattering source. For the thinnest film (20 nm), the superfluid density has no influence on the transmission coefficient down to temperatures well below T_c. Therefore the temperature dependence of the transmission is completely determined by σ_1, even at temperatures down to 60 K. The thicker films show a more conventional behaviour, where ϵ' indeed dominates the transmission in most of the superconducting range.

Acknowledgements

We gratefully acknowledge stimulating discussions with W.N. Hardy and the technical support of C.J. Bos and W.A. Schoonveld.

References

[1] W.N. Hardy, D.A. Bonn, D.C. Morgan, R. Liang, K. Zhang, Phys. Rev. Lett. 70 (1993) 3999.
[2] D.H. Wu, J. Mao, S.N. Mao, J.L. Peng, X.X. Xi, T. Venkatesan, R.L. Greene, S.M. Anlage, Phys. Rev. Lett. 70 (1993) 85.
[3] K. Zhang, D.A. Bonn, S. Kamal, R. Liang, D.J. Baar, W.N. Hardy, D. Basov, T. Timusk, Phys. Rev. Lett. 73 (1994) 2484.
[4] J. Annet, N. Goldenfeld, S.R. Renn, Phys. Rev. B 43 (1991) 2778.
[5] D.A. Wollman, D.J. van Harlingen, W.C. Lee, D.M. Ginsberg, A.J. Legget, Phys. Rev. Lett. 71 (1993) 2134.
[6] J.R. Kirtley, C.C. Tsuei, J.Z. Sun, C.C. Chi, L.S. Yu-Jahnes, A. Gupta, M. Rupp, M.B. Ketchen, Nature 373 (1995) 225.
[7] Z.-X. Shen, D.S. Dessau, B.O. Wells, D.M. King, W.E. Spicer, A.J. Arko, D. Marshall, L.W. Lombardo, A. Kapitulnik, Phys. Rev. Lett. 70 (1993) 1553.
[8] T.E. Mason, G. Aeppli, S.M. Hayden, A.P. Ramirez, H.A. Mook, Phys. Rev. Lett. 71 (1993) 919.
[9] T.P. Devereaux, D. Einzel, B. Stadtlober, R. Hackl, D.H. Leach, J.J. Neumeier, Phys. Rev. Lett. 72 (1994) 396.
[10] N. Klein, U. Dähne, U. Poppe, N. Tellmann, K. Urban, S. Orbach, S. Hensen, G. Müller, H. Piel, J. Supercond. 5 (1992) 195.
[11] A.T. Fiory, A.F. Hebard, P.M. Mankiewich, R.E. Howard, Phys. Rev. Lett. 61 (1988) 1419.
[12] M.R. Beasley, Physica C 209 (1993) 43.
[13] Z. Ma, R.C. Taber, L.W. Lombardo, A. Kapitulnik, M.R. Beasly, P. Merchant, C.B. Eom, S.Y. Hou, J.M. Philips, Phys. Rev. Lett. 71 (1993) 781.
[14] P.J. Hirschfeld, N. Goldenfeld, Phys. Rev. B 48 (1993) 4219.
[15] J. Halbritter, Phys. Rev. B 48 (1993) 9735.

[16] L.A. de Vaulchier, J.P. Vieren, Y. Guldner, N. Bontemps, R. Combescot, Y. Lemaître, J.C. Mage, Europhys. Lett. 33 (2) (1996) 153.
[17] D.A. Bonn, P. Dosanjh, R. Liang, W.N. Hardy, Phys. Rev. Lett. 68 (1992) 2390.
[18] M.C. Nuss, P.M. Mankiewich, M.L. O'Malley, E.H. Westerwick, P.B. Littlewood, Phys. Rev. Lett. 66 (1991) 3305.
[19] F. Gao, Y. Liu, J.W. Kruse, J.F. Whitaker, C.E. Platt, M. Feng, M.V. Klein, Appl. Phys. Lett. 63 (16) (1993) 2274.
[20] K. Holczer, L. Forro, L. Mihály, G. Grüner, Phys. Rev. Lett. 67 (1991) 152.
[21] O. Klein, E.J. Nicol, K. Holczer, G. Grüner, Phys. Rev. B 50 (1995) 6307.
[22] D.A. Bonn, S. Kamal, K. Zhang, R. Liang, D.J. Baar, E. Klein, W.N. Hardy, Phys. Rev. B 50 (1994) 4051.
[23] T. Nagashima, S. Harada, M. Hangyo, S. Nakashima, M Mukaiada, S. Miyazawa, Physica C 271 (1996) 365.
[24] Z.H. Barber, M.G. Blamire, R.E. Somekh, J.E. Evetts, IEEE Trans. Supercond. 3 (1993) 2054.
[25] U. Dähne, Y. Goncharov, N. Klein, N. Tellmann, G. Kozlov, K. Urban, J. Supercond. 8 (1995) 129.
[26] M. Tinkham, Introduction to Superconductivity, McGraw-Hill, New York, 1975 and Krieger, New York, 1980.
[27] D.C. Mattis, J. Bardeen, Phys. Rev. 111 (1958) 412.
[28] A. Shoji, S. Kiryu, S. Kohjiro, Appl. Phys. Lett. 60 (13) (1992) 1624.